Physics Procedia
Volume 75, 2015, Pages 1376–1380
20th International Conference on Magnetism

Structural heterogeneity of the melt-spun (Fe, Co)-Si-B-P-Cu alloy with excellent soft magnetic properties

Kazuhisa Sato[1*], Kana Takenaka[1], Akihiro Makino[1] and Yoshihiko Hirotsu[2]
[1]*Institute for Materials Research, Tohoku University, Sendai, Japan*
[2]*Institute of Scientific and Industrial Research, Osaka University, Ibaraki, Japan*

Abstract
A structural heterogeneity of a newly developed soft magnetic $Fe_{81.2}Co_4Si_{0.5}B_{9.5}P_4Cu_{0.8}$ melt-spun alloy has been studied by transmission electron microscopy (TEM) and electron diffraction. Hollow-cone dark-field TEM imaging revealed that the density of coherent scattering regions in the as-quenched $Fe_{81.2}Co_4Si_{0.5}B_{9.5}P_4Cu_{0.8}$ alloy is as high as that in the $Fe_{85.2}Si_2B_8P_4Cu_{0.8}$ hetero-amorphous alloy (NANOMET®). According to the aberration-corrected high-resolution TEM, crystalline atomic clusters, typically of ~1 nm in diameter, are densely distributed in an amorphous matrix of $Fe_{81.2}Co_4Si_{0.5}B_{9.5}P_4Cu_{0.8}$ alloy, while nanobeam electron diffraction detected weak Bragg reflections from Fe clusters with the body centered cubic structure. These results unambiguously reveal structural heterogeneity of the as-quenched $Fe_{81.2}Co_4Si_{0.5}B_{9.5}P_4Cu_{0.8}$ alloy, which is similar to that observed in the NANOMET®.

Keywords: Structural heterogeneity, Hetero-amorphous, Fe cluster, Soft magnetic material, NANOMET

1 Introduction

Nanocrystalline soft magnetic materials originated from Fe-based amorphous alloys have been developing for long years by tuning alloy composition and constituent elements [1-3]. The FeSiBPCu nanocrystalline soft magnetic alloy (NANOMET®) contains more than 83at%Fe, and is known to exhibit excellent soft magnetic properties with a high saturation magnetization after a proper heat treatment of an as-quenched ribbon (H_c = 7-10 A/m, B_s = 1.88-1.94 T) [4, 5]. The excellent soft magnetic properties of the FeSiBPCu nanocrystalline alloy can be attributed to the high-density α-Fe nanocrystals as well as the high Fe content exceeding 80at%. “Pre-existing” Fe clusters formed at the as-quenched state could act as nucleation sites for the Fe grains with the body centered cubic (bcc) structure during the crystallization of hetero-amorphous structure [4, 6]. Actually, our recent study has revealed the presence of crystalline atomic clusters in a melt-spun $Fe_{85.2}Si_2B_8P_4Cu_{0.8}$ alloy [7].

[*]Corresponding author. Tel: +81-22-215-2159; fax: +81-22-215-2159
E-mail address: ksato@imr.tohoku.ac.jp

 Selection and peer-review under responsibility of the Scientific Programme Committee of ICM 2015

doi:10.1016/j.phpro.2015.12.154

Recently, Takenaka et al. have reported that significant low H_c (7 A/m) and sufficiently high B_s (1.84 T) can be obtained simultaneously even in a thicker ribbons exceeding 30 μm in thickness when small amount of Fe is replaced by Co [8]. According to their preceding study [8], the best soft magnetic properties are achieved in the nanocrystalline $Fe_{81.2}Co_4Si_{0.5}B_{9.5}P_4Cu_{0.8}$ alloy. It is also noted that they have succeeded in fabricating a melt-spun ribbon in air with 50 mm in width, ~65 m in length, and ~25 μm in thickness. The production of wide and thick ribbons is indispensable for commercial applications of the nanocrystalline alloy to power transformers and motors.

The purpose of this study is to reveal atomic structures of a newly developed melt-spun (Fe, Co)-Si-B-P-Cu alloy using spherical aberration (C_s) corrected high-resolution transmission electron microscopy (HRTEM) and electron diffraction. In addition to highly improved spatial resolution (~0.1 nm), C_s-corrected HRTEM has a benefit of smaller defocus values under optimal defocus condition, which is beneficial for imaging extremely small atomic clusters [9].

2 Experimental

Alloy ingots of FeCoSiBPCu were prepared by induction melting of Fe (99.9 mass%), Co (99.5 mass%), Si (99.999 mass%), B (99.5 mass%), Cu (99.99 mass%) and premelted Fe_3P (99 mass%) in a high purity argon (Ar) atmosphere. Rapidly solidified FeCoSiBPCu ribbons with 10 mm in width and ~20 μm in thickness were prepared using the aforementioned ingots by a single-roller melt-spinning method in air [8]. Plan-view TEM specimens were prepared by a mechanical polishing in ethanol using a 0.3 μm-Al_2O_3 wrapping film followed by a low voltage Ar-ion milling at low temperatures (~180 K). For atomic structure imaging using a 300 kV-TEM (FEI TITAN80-300), the C_s value was adjusted to approximately 8 μm. In the present experimental condition, theoretical optimal defocus required for atomic structure imaging is as small as 4.6 nm, which can effectively minimize imaging artifact. Possible structural change due to electron irradiation can be excluded in the HRTEM observation using a CCD camera with a short acquisition time of 1 s or less [9]. Nanobeam electron diffraction (NBED) patterns were obtained by scanning ~0.5 nm-sized electron probe using a 200 kV-TEM with a cold field emission gun (JEOL JEM-ARM200F). A beam convergence semi-angle was set to ~3 mrad in the NBED experiments using a condenser aperture of 5 μm in diameter.

3 Results and discussion

A hollow-cone dark-field (DF) TEM image is shown in Fig. 1(a) for a newly developed melt-spun $Fe_{81.2}Co_4Si_{0.5}B_{9.5}P_4Cu_{0.8}$ alloy. An attached selected area electron diffraction (SAED) pattern obtained from a wide area (~700 nm in diameter) shows only halo rings arising from amorphous structure. Diffracted waves contributing to the first halo ring were selected by a small objective aperture (10 μm in diameter) and were employed for the hollow-cone DF-TEM imaging. In this procedure, the incident electron beam was deflected by ~7 mrad in the radial direction and then rotated in the circumference direction. Thus, all the intensity from the first halo ring was incorporated with an on-axis DF-TEM image. In Fig. 1(a), bright contrast so called “speckle” is considered to come from atomic medium-range order (MRO) in the amorphous structure [10, 11]. For comparison, hollow-cone DF-TEM images and the corresponding SAED patterns of an as-quenched $Fe_{85.2}Si_2B_8P_4Cu_{0.8}$ hetero-amorphous alloy and an $Fe_{76}Si_9B_{10}P_5$ bulk metallic glass with single amorphous phase are also shown in Fig. 1(b) and 1(c), respectively. The areal number density of strong speckled-contrasts of FeCoSiBPCu is comparable to that of FeSiBPCu hetero-amorphous alloy, but is obviously higher than that of the bulk metallic glass. Thus DF-TEM imaging clearly reveals the presence of a highly heterogeneous structure of atomic clusters (MRO regions) in the FeCoSiBPCu alloy, as observed in the FeSiBPCu hetero-amorphous alloy. This is in good agreement with the results based on thermal analysis reported in the preceding study [8]. To clarify the atomic structure of such high-density speckles, we have performed the C_s-corrected TEM observation.

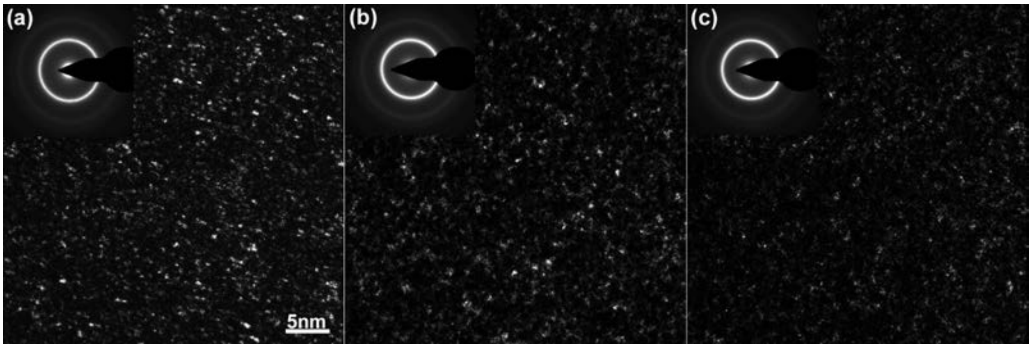

Figure 1: Hollow-cone DF-TEM images and the corresponding SAED patterns of as-quenched ribbons: (a) a newly developed $Fe_{81.2}Co_4Si_{0.5}B_{9.5}P_4Cu_{0.8}$ alloy, (b) an $Fe_{85.2}Si_2B_8P_4Cu_{0.8}$ hetero-amorphous alloy and (c) an $Fe_{76}Si_9B_{10}P_5$ bulk metallic glass.

Figure 2 shows a C_s-corrected HRTEM image of an as-quenched $Fe_{81.2}Co_4Si_{0.5}B_{9.5}P_4Cu_{0.8}$ alloy. Small atomic ordered regions are observed in the encircled area. There is a size distribution of such local ordered regions ranging from 1 nm to about 2 nm. An ordered region of bright spots appearing in the HRTEM image of amorphous alloy under a suitable imaging condition comes from a local atomic ordered region in the alloy [12, 13]. In this alloy, deformed images of ordered regions are often seen as shown in the white bold-circles. Also, we often observe eucentric onion-like contrasts (see in the white thin circle with a single arrowhead). In the local image regions of deformed clusters, we sometimes observe regions of four-fold-like and six-fold-like clusters (as indicated by the letters “a” and “b” in the figure, respectively), implying possible existence of local crystalline bcc-Fe clusters [14]. The smallness of such ordered regions and their deformation draw our attention in this Co-added alloy in comparison with those in NANOMET®. It should be noted that, according to the preceding image simulation studies, such locally ordered regions are not reproduced by assuming a dense random packing (DRP) model structure [12, 13, 15]. A rigorous image simulation [16] has to be made for such characteristic types of local crystalline clusters (including the onion-like clusters) in order to understand the observed important images of local clusters. We have obtained similar HRTEM images for an as-quenched $Fe_{81.2}Co_4Si_{0.5}B_{9.5}P_4Cu_{0.8}$ ribbon with 50 mm in width and ~25 μm in thickness.

Figure 3 shows scanning NBED patterns including weak diffraction spots. The pattern shown in Fig. 3(a) is close to $\sim[001]_{bcc\text{-}Fe}$ zone-axis pattern. Reflections indicated by arrowheads having a lattice spacing of ~0.2 nm correspond to 110 reflections of bcc-Fe. A NBED pattern shown in Fig. 3(b) is close to the pattern of $\sim[111]_{bcc\text{-}Fe}$ zone composed of six-fold $110_{bcc\text{-}Fe}$ reflections. Thus, the observation of these NBED patterns is also a strong evidence of existence of crystalline bcc-Fe clusters in the as-quenched melt-spun $Fe_{81.2}Co_4Si_{0.5}B_{9.5}P_4Cu_{0.8}$ ribbon. It should be noted that these NBED patterns from the cluster regions are usually deformed and asymmetric in their spot-intensities with respect to the central spot due to their local lattice distortion. The distortion of interplanar spacing (spot distance) derived from the NBED patterns is at most ~8%. Namely, there is a distribution in interplanar spacing and some of the clusters are heavily distorted. Also note that background noise seen in the NBED patterns come from weak scattering by several atomic clusters in amorphous matrix surrounding crystalline clusters. Sharma et al. have proposed that the pre-existing nuclei and the newly formed nuclei in the annealing process will grow together [6]. It is presumed that among the dense atomic clusters exist in the as-quenched alloy a part of the clusters with structures close to the bcc-Fe must contribute to high-density α-Fe nanocrystals produced by post-annealing. It has been reported that additive Co was detected in α-Fe grains after crystallization based on elemental mapping using energy dispersive x-ray spectrometry (EDX) [8]. Overall, we have confirmed that structural features of the newly developed $Fe_{81.2}Co_4Si_{0.5}B_{9.5}P_4Cu_{0.8}$ alloy are almost similar to those observed in the $Fe_{85.2}Si_2B_8P_4Cu_{0.8}$ hetero-amorphous alloy (NANOMET®).

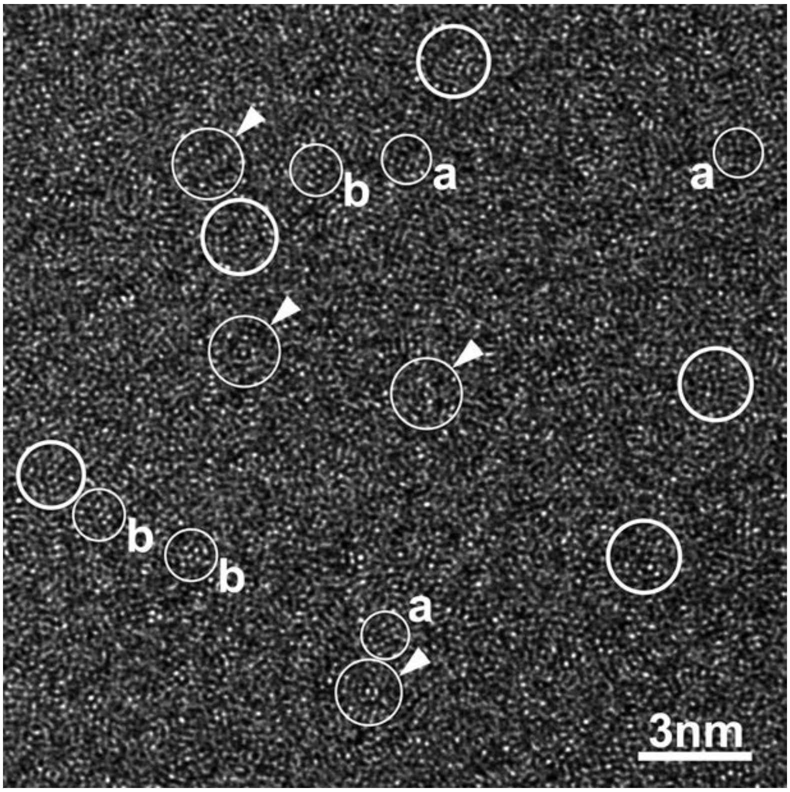

Figure 2: C_s-corrected HRTEM image of an as-quenched $Fe_{81.2}Co_4Si_{0.5}B_{9.5}P_4Cu_{0.8}$ alloy. Atomic clusters are seen in the encircled area. The letters “a” and “b” indicate four-fold-like and six-fold-like crystalline atomic clusters, respectively. Heavily deformed images of ordered regions are seen in the bold-circles. Arrowheads indicate eucentric “onion-like” contrasts.

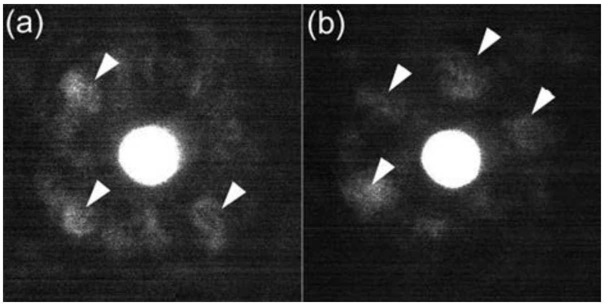

Figure 3: Scanning NBED patterns including weak diffraction spots. Probe size is ~0.5 nm with beam convergence semi-angle of ~3 mrad. Beam incidence ~$[001]_{bcc\text{-}Fe}$ (a) and ~$[111]_{bcc\text{-}Fe}$ (b). Arrowheads indicate 110 reflections of bcc-Fe.

4 Summary

In summary, a combination of C_s-corrected HRTEM and scanning NBED unambiguously revealed a structural heterogeneity including high-density crystalline atomic clusters as small as 1 nm in the as-quenched $Fe_{81.2}Co_4Si_{0.5}B_{9.5}P_4Cu_{0.8}$ alloy. A part of these clusters is bcc-Fe-like in respect of lattice spacing and symmetry of NBED patterns as well as atomic image contrast. The structural features observed in the $Fe_{81.2}Co_4Si_{0.5}B_{9.5}P_4Cu_{0.8}$ alloy are almost similar to those observed in the $Fe_{85.2}Si_2B_8P_4Cu_{0.8}$ hetero-amorphous alloy. In other words, by replacing a small amount of Fe with Co, a production of wider and thicker ribbon is possible without any characteristic change of structural details as well as soft magnetic properties of NANOMET®.

Acknowledgements

This work was supported by the “Tohoku Innovative Materials Technology Initiatives for Reconstruction (TIMT)” funded by the Ministry of Education, Culture, Sports, Science and Technology (MEXT) and Reconstruction Agency, Japan. KS wishes to thank Prof. N. Nishiyama, Dr. P. Sharma and Dr. A. Hirata of Tohoku University for invaluable comments.

References

[1] Y. Yoshizawa, S. Oguma, K. Yamauchi, J. Appl. Phys. 64 (1988) 6044.
[2] K. Suzuki, A. Makino, N. Kataoka, A. Inoue, T. Masumoto, Mater. Trans. JIM 32 (1991) 93.
[3] M. A. Willard, D. E. Laughlin, M. E. McHenry, D. Thoma, K. Sickafus, J. O. Cross, V. G. Harris, J. Appl. Phys. 84 (1998) 6773.
[4] A. Makino, H. Men, T. Kubota, K. Yubuta, A. Inoue, Mater. Trans. 50 (2009) 204.
[5] A. Makino, H. Men, T. Kubota, K. Yubuta, A. Inoue, J. Appl. Phys. 105 (2009) 07A308.
[6] P. Sharma, X. Zhang, Y. Zhang, A. Makino, Scripta Mater. 95 (2015) 3.
[7] K. Sato, K. Takenaka, A. Makino, Y. Hirotsu, AIP Advances 5 (2015) 067166.
[8] K. Takenaka, A. D. Setyawan, Y. Zhang, P. Sharma, N. Nihsiyama, A. Makino, Mater. Trans. 56 (2015) 372.
[9] K. Sato, M. Mizuguchi, R. Tang, J. –G. Kang, M. Ishimaru, K. Takanashi, T. J. Konno, Appl. Phys. Lett. 101 (2012) 191902.
[10] M.-H. Kwon, B.-S. Lee, S. N. Bogle, L. N. Nittala, S. G. Bishop, J. R. Abelson, S. Raoux, K.-B. Kim, Appl. Phys. Lett. 90 (2007) 021923.
[11] M. M. J. Treacy, J. M. Gibson, L. Fan, D. J. Paterson, I. McNulty, Rep. Prog. Phys. 68 (2005) 2899.
[12] Y. Hirotsu, T. Ohkubo, and M. Matsushita, Microsc. Res. Tech. 40 (1998) 284.
[13] A. Hirata, Y. Hirotsu, T. Ohkubo, T. Hanada, V. Z. Bengus, Phys. Rev. B 74 (2006) 214206.
[14] Y. Hirotsu and R. Akada, Jpn. J. Appl. Phys. 23 (1984) L479.
[15] T. Hamada and F. E. Fujita, Jpn. J. Appl. Phys. 25 (1986) 318.
[16] M. Aykol, A.O. Mekhrabov, M.V. Akdeniz, Acta Mater. 57 (2009) 171.